Inter-Research Science Publisher

Aquaculture Environment Interactions
Volume 17:1–20

Published January 23, 2025
https://doi.org/10.3354/aei00489

Disaggregation rates of salmon feces and microbial inoculation of sediments: new insight for particle dispersion modelers

Nigel Keeley[1,*], Katherine Dunlop[1], Olivier Laroche[2], Ellie Watts[1], Pål Sævik[3], Jon Albretsen[3]

[1]Institute of Marine Research, Framsenteret, PO Box 6606 Langnes, 9296 Tromsø, Norway
[2]Cawthron Institute, Private Bag 2, Nelson 7040, New Zealand
[3]Institute of Marine Research, PO Box 1870 Nordnes, 5817 Bergen, Norway

ABSTRACT: The flow of organic waste into the environment from large-capacity fish farms, and its consequences for the marine ecosystem, is a contentious issue. Our ability to manage and mitigate the effects can be improved by enhancing our ability to predict dispersal and distribution of waste, and by better understanding the mechanisms that drive ecological perturbation. This study examines the fate of individual particles in controlled chambers, designed to simulate contrasting receiving environments, and the ensuing physical, chemical, and microbial changes. Fecal particles that landed on impacted sediments broke down twice as fast as those on natural sediments and were effectively removed from the system after 160 h, which was attributed to microbe- and fauna-mediated decomposition. Particles in turbulent water disaggregated rapidly into numerous smaller particles, which persisted for >200 h. These smaller particles have fundamentally different physical properties, which, when included in dispersion models, increase the predicted horizontal dispersion and flux rates at distances >1 km and the potential for overlapping effects between farms. Microbial inoculation of the sediment from waste particles was limited, but evident, especially for natural sediments, which were significantly altered from a single introduction of fecal pellets at a density of 288 to 481 m^{-2}. Therefore, waste-dispersion models may be improved by the inclusion of particle breakdown stages with associated size-specific behavioral dynamics and benthic impact-specific sediment consolidation times. Further consideration should be given to the potential for the microbiome of the receiving environment to be altered by extraneous sources, both near and far field.

KEY WORDS: Biodeposition · Decomposition · Microbial eDNA · Benthic impacts · Organic enrichment · Waste dispersion

1. INTRODUCTION

Salmon farms produce significant quantities of waste particulates, primarily in the form of fish feces, which induce pronounced ecological effects on the underlying seabed, easing in intensity with increasing distance. For typical farms situated in moderate- to low-flow environments, the effects are usually acute and can be associated with anoxic sediments with severely compromised life-supporting capacity, but which rapidly grade to near natural conditions within a relatively short distance (i.e. 100–200 m away from farm cages) (Brooks & Mahnken 2003, Borja et al. 2009, Papageorgiou et al. 2010). In contrast, farms situated in deep water or with stronger hydrodynamics can have considerably larger, more

*Corresponding author: nkeeley@hi.no

Publisher: Inter-Research · www.int-res.com

diffuse footprints with effects observable up to 1 km from the fish structures (Kutti et al. 2007, Keeley et al. 2019). Understanding the size, shape, and characteristics of these ecological effect footprints is an important aspect of environmental sustainability and for planning and managing aquaculture installments, especially with respect to avoiding potentially overlapping footprints and adversely affecting ecologically important or sensitive habitats.

It has been possible to predict the approximate spatial extent and magnitude of benthic effects from salmon farms for approximately 20 yr with the combined use of hydrodynamic and particle dispersion models (Cromey et al. 2000, Broch et al. 2017, Smeaton & Vennell 2020). However, early versions of the models were necessarily simplistic, making assumptions that introduced uncertainty and potential errors. As a result, the approach to depositional modeling has undergone constant evolution on many fronts, including improving the way certain physical processes are managed (Keeley et al. 2013b, Law et al. 2016, Adams et al. 2020, Carvajalino-Fernández et al. 2020b), such as increasing model sophistication and spatial resolution (Smeaton & Vennell 2020, Hartstein et al. 2021, Vennell et al. 2021) and refining important input parameters (Chen et al. 2003, Chamberlain & Stucchi 2007, Law et al. 2014, Bannister et al. 2016) and erosion coefficients (Fox et al. 2023). Although increasingly sophisticated, these models still lack reliable estimates for some key parameters, and several unresolved issues remain (Fox et al. 2023).

One such weakness concerns the structural integrity of the particles and knowledge of the effective lifespan for a particle in simulations (Magill et al. 2006, Carvajalino-Fernández et al. 2020b). Until recently, most models assumed that particles are a single size and maintain their initial dimension through time, either perpetually (conserved) or until such a point that they are terminated within the model (simulating sudden decay, breakup, and/or consumption). This is despite the fact that particles represent a range of sizes and, therefore, settling velocities, which has important implications for horizontal advection ranges (Bannister et al. 2016). At one extreme, if the particles are conserved and continually released, then the model produces a continually expanding footprint, i.e. the longer the model runs, the larger the footprint. Conversely, if particles are removed from the model after a relatively short time (e.g. 24 h), then this drastically constrains the possible footprint size. At present, particle lifespan is either ignored (Cromey et al. 2012, Broch et al. 2017, Adams et al. 2020), arbitrarily constrained by the number of timesteps in the model (e.g. Magill et al. 2006), conservatively estimated to ensure worst-case scenarios are anticipated (e.g. 12 d, Carvajalino-Fernández et al. 2020b), or inferred from measurements of carbon decay rates (Fox et al. 2023). There are no actual measurements of the nature and rapidity of particle breakup. Moreover, if particles break apart rapidly into a much greater number of smaller particles, or conversely, aggregate into flocs (e.g. Law et al. 2014), this will presumably have a profound effect on their physical properties and therefore, horizontal dispersion. Most, if not all, fish farm particle dispersion models currently assume that the physical properties of the particles do not change. The first aim of this study was therefore to characterize the breakdown process of salmon fecal particles in various seafloor environments to improve our ability to predict dispersal and distribution of waste in models.

The second part of this study aims to consider the influence that these waste particles have when they eventually reach the seabed subsequent to physical dispersion. While the biological and geochemical changes in response to organic enrichment are reasonably well described (Hargrave et al. 2008), and some approximate relationships between depositional flux and benthic effects have been established (Keeley et al. 2013b), there has been very little focus on the potential for inoculation of the benthic environment with fish farm-sourced microbiota. Several studies have demonstrated the establishment of strong microbial gradients with proximity to fish farms, with microbial communities beneath farms being vastly different from those found in natural sediments (Pochon et al. 2015, Keeley et al. 2018, Stoeck et al. 2018, Frühe et al. 2021). Microbial communities are implicit in benthic functioning and, in particular, the geochemical processes associated with metabolizing organic waste (McCaig et al. 1999, Jørgensen et al. 2019). As such, it is generally assumed that contrasting bacterial communities are tightly coupled to, and a consequence of, the enrichment process (Kawahara et al. 2009). This is supported by the fact that the microbes that characterize the benthic flora in impacted sediments beneath fish farms appear to be reasonably universal (Frühe et al. 2021, Keeley et al. 2021). However, it is also conceivable that salmon fed a standardized diet will produce feces with a characteristic microbiome and, given sufficient inoculation pressure (i.e. from biodeposition), may be at least partially responsible for the microbial alterations that are being observed. It is therefore presently unclear which process is more responsible for the observed changes — the 'bottom-up' enrichment process, or

the 'top-down' inoculation — and, if it is the latter, what consequence does this flux of 'non-native' microbes have on the receiving environment? Furthermore, it is not known how much inoculation pressure is required to have an influence.

To address some of these deficiencies, we conducted a laboratory study wherein particle breakup and decay rates of salmon feces were evaluated on 2 contrasting types of sediment (natural and highly enriched), on an inert plastic substrate with static seawater, and when suspended and constantly moving in turbulent seawater in chambers. Measurements were taken with the aid of visual and image-recognition techniques over a prescribed period. The potential for microbial inoculation of the sediments was assessed via 16S metabarcoding of the feces, seawater, and sediments before and after the feces were introduced. The results from both parts of this trial are discussed herein, and the implications of the observed particle dynamics are shown with particle dispersal model simulations.

2. MATERIALS AND METHODS

2.1. Particle breakup and decay experiments

2.1.1. Sourcing of sediments and fish feces

Two contrasting types of sediments were collected by van Veen grab. One type was from a highly enriched area of seabed beneath a recently fallowed salmon farm in Vengsøyfjorden in northern Norway. These sediments were visually blackened and highly organically enriched with a strong hydrogen sulfide odor. The second sediment type was collected from a similar depth in a nearby sound that contained no fish farms, and was muddy and natural in appearance, grey-brown in color, with no noticeable sulfide odor. Upon retrieval, the sediments were immediately transferred to the experimental chambers and placed in a tray with flow-through seawater to maintain sea temperature and shielded from direct sunlight for transportation to the laboratory. In the laboratory, the chambers were set up in rows, each with an independent water supply from 5 mm silicone tubing regulated by a valve supplying flow rates of approximately 100 ml min^{-1}, which was sufficient to gently exchange the water to avoid anoxia, but not resuspend any sediment. The chambers were left to settle and acclimatize for 24 h before the experiments commenced.

Fecal pellets were sourced from approximately 50 Atlantic salmon *Salmo salar* (~1 kg, 40–45 cm) cultured in land-based tanks and fed on standard Spirit 4.5 mm salmon pellets from Skretting AS. Fish were anesthetized using AQUI-S before feces were extruded from the gut into sample jars. The feces were transferred immediately to the experimental chambers where the largest, most cohesive, and bound particles were sorted out and extracted from the slurry with an adapted syringe siphon.

2.1.2. Experimental design

Impacted marine sediment was sourced from a recently fallowed salmon farm close to the net pens and was clearly highly organically enriched (i.e. black, anaerobic, strong sulfide odor, traces of white bacteria on surface). Natural sediments were sourced from a site with similar depths and sediment in a neighboring area of the fjord >2 km from any obvious anthropogenic discharges.

A total of 30 individually numbered incubation chambers were used to monitor the breakdown rates of fecal particles in 4 different environments: (1) on natural sediments ('Natural'); (2) on highly enriched sediments ('Impacted'); (3) with no sediment, on a perforated plastic base ('Static'); and (4) held in suspension in a turbulent environment ('Turbulent'). Each treatment comprised 5 replicate chambers, each with an independent water supply from a common source (drawn from 100 m depth in a neighboring fjord, temperature 10–12°C), and outgoing water was not recycled. For the 2 treatments involving sediment, an additional 5 chambers were used for each sediment type as controls for the microbial study, which did not receive feces. Thus, the 6 treatments were (1) Natural, (2) Natural + feces, (3) Impacted, (4) Impacted + feces, (5) Static, and (6) Turbulent (Fig. 1). All but the Turbulent treatment remained largely undisturbed (with the exception of the periodic 'integration test'; see Section 2.1.3) to allow the natural decay and breakdown process to occur, while the Turbulent treatment was constantly subjected to an upwelling flow (through a perforated base and top-plate to retain the particles) to keep the particles moving and held in suspension to simulate a physically dynamic receiving environment.

The chambers comprised 2 l plastic low-density polyethylene flasks (KJS brand), 11.5 cm in diameter, with the bottom removed and inverted. Perforated plastic disks (1.5 mm holes) were inserted at the tapered base of each inverted flask in the Static and Turbulence treatment chambers, which served as the base substrate for the fecal pellets. In the case of the sediment-loaded tubs, a 12 cm depth of either natural or

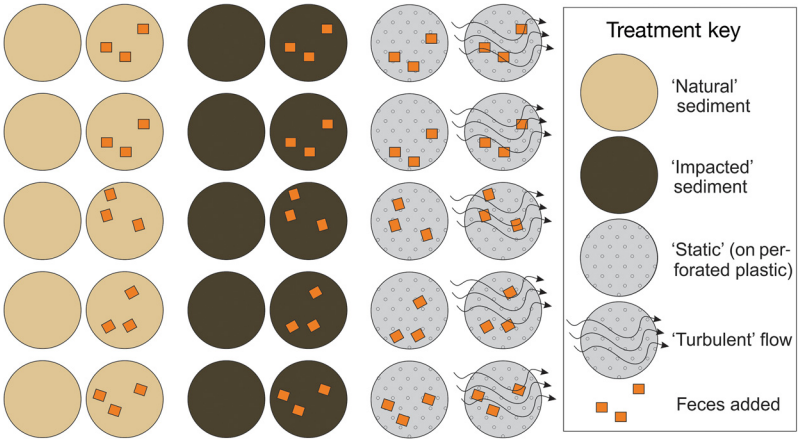

Fig. 1. Basic experimental set-up indicating arrangement of treatment chambers, feed additions, and flow regimes

impacted sediment was placed in the bottom of the chamber. All treatments received a 'maintenance flow' of ambient-temperature sea water measured daily, filtered to 60 µm. Water was delivered to each flask via a 30 mm polyethylene pipe manifold with individual 5 mm silicon tubing placed halfway down the wall of each flask for top-down gentle circulation. Flow rate was controlled via a plastic screw valve, with a rate averaging approximately 100 ml min^{-1}. A clear 4 cm piece of 5 mm diameter plastic tube with 1 cm increments was placed on the sediment or sieve surface in each flask as a scale bar for the photographs.

Approximately 3 fecal particles were gently released into the bottom of the appropriate sample chambers at the start of the trial. Obtaining large, similarly sized fecal pellets proved difficult so, in some cases, the particles were of variable sizes.

2.1.3. Sampling procedure

Particle breakup was tracked with still photos of the surface of each chamber at a frequency that reduced over time; from hourly intervals for the first 7 h, then every 2 h for the next 15 h, then every 6 h for 2 d, and then approximately daily until the conclusion of the experiment. The 4 treatments were concluded at different times dependent on when the particles were assessed to be sufficiently decayed, as follows: Impacted sediments 210 h, Natural sediments 240 h, Static seawater 350 h, and Turbulent chambers 160 h. Still photos were taken using an Olympus Tough TG-5 camera at 4 mm focal length lens set to ISO 100, 1/100 s exposure and *f*-stop with side lighting through the semi-transparent (diffuse) chamber walls, where the camera was positioned in the same location (20 cm above and perpendicular to the top of the chamber, thereby setting focal length). The internal clock of the camera was used to track exact timing, and a photo was taken of the chamber number prior to photographing the surface to assist record keeping.

Additionally, observations were recorded regarding pellet cohesiveness, whether they were sticking to the surface (plastic or sediment) or were freely resuspended. Every 24 h at around 09:00 h, each particle in the Static, Control and Impacted sediment treatments (i.e. not in the Turbulent treatment) was subjected to a controlled disturbance (hereafter termed 'disturbance'). To do this, 40 ml of seawater were drawn from the resident chamber using a modified syringe with a large 6 mm aperture. The contents of the syringe were then plunged out in a slow and controlled manner, with the water flow directed in a slow swirling pattern for 1–2 s to gently disturb the sediment surface around the pellets. The objective was to test if a particle could be easily dislodged and still cohesive (not prone to breakdown by natural turbulence); the jetting was not strong enough to move the particles substantively, or cause turbulence within the chamber. At the same time, observations were also made regarding the presence and behavior of any fauna activity and/or visual bacterial formation. The syringe was repeatedly rinsed with reverse osmosis water between chambers.

2.1.4. Image analyses procedure

Images were viewed in Adobe Photoshop CC 2020 and analyzed to obtain fecal pellet counts, a measurement of the surface area of each fecal pellet, as well as the total surface area covered by pellets. Prior to analysis, the light and color distributions of the images were adjusted using batch processing methods to enable the automated color sampling tools to be applied. The color range tool was used to select all fecal pellets, which were similar color and in contrast to the grey background. The count tool was selected in 'Image > Analysis' and the measurement scale was set to 1 cm using the scale bar in the image. Subsequently, a measurement log was recorded of fecal pellet number, the area of each pellet and the total area of the image covered by pellets. The workflow was recorded using action files which, once applied to one image, could be automatically applied to the whole

sequence of images. Data were assessed according to the physical composition of the particles at the start of the experiment when peak particle abundance occurred, the main breakup phase and the end point, which was determined when size, count, and total area reached <20% of the start number.

2.2. Sediment analyses and microbial inoculation

Microbial inoculation of the sediments resulting from introducing fecal pellets was assessed via 10 additional chambers containing Impacted and Natural sediments (i.e. 5 replicates of each) that did not receive feces and therefore served as reference chambers. Prior to introducing the fecal pellets and again at the conclusion of the experiment, each chamber was non-destructively sampled to assess the organically enriched status of the sediments. Redox potential and pH were measured at 2 haphazardly selected positions on the surface of each chamber (5–10 mm deep) using an HI98191 meter (Hanna Instruments) with an HI1296 pH/ORP/°C electrode probe. Sediment total free sulfide ($S^{2-}{}_{UV}$, μM) was evaluated directly from triplicate haphazardly selected positions from each chamber, following the direct ultraviolet spectrophotometry method of Cranford et al. (2020). At the conclusion of the experiment, the sediment chambers were sieved out and the fauna retained on a 1 mm mesh was preserved with buffered ethanol for full taxonomy by macroscopy. All conspicuous fauna were sorted, identified to the lowest possible taxonomic level, and enumerated by appropriately trained local taxonomists. Macrofauna bioinformatics S (total number of taxa), N (total number of individuals), AMBI (AZTI's marine biotic index; Borja et al. 2000), and Norwegian Sensitivity Index (NSI, Rygg & Norling 2013) were calculated from the count data using the 'BBI' package (v0.3.0) in R. The estimated marginal means for each variable were obtained from the associated 'lm' or 'lmer' models using the 'emmeans' package, and the pairwise significances were displayed on corresponding scatterplots using 'ggplot.'

2.3. Microbial eDNA analyses

Triplicate 5 g samples of sediment were taken, using clean disposable teaspoons, from the top of each sediment chamber before and after the trials and stored in Eppendorf tubes. The 'Before' samples were taken from randomly selected locations prior to introducing the feces, while the 'After' samples were taken at semi-randomly selected locations, avoiding sampling directly on top of any residual fecal pellets. Samples were transferred to a −80°C freezer within 1 h of being collected for storage.

2.3.1. DNA extraction and targeted 16S rRNA library preparation

Sediment samples were processed with the Qiagen DNeasy Powersoil Kit using 0.25 g of sediment and following the manufacturer's instructions. Negative controls were included throughout the extraction process by replacing sediment with double-distilled water (ddH_2O).

A 2-step PCR approach was applied to all samples using the universal forward primer S-D-Bact-0341-b-S-17: 5'-CCT ACG GGN GGC WGC AG-3' and reverse primers S-D-Bact-0785-a-A-21: 5'-GAC TAC HVG GGT ATC TAA TCC-3' (Klindworth et al. 2013) for amplification of a short (ca. 400–450 bp) fragment of the nuclear 16S rRNA bacterial gene (V3–V4 region). The universal primers were modified to include Illumina™ forward and reverse overhang adaptors (5'-TCG TCG GCA GCG TCA GAT GTG TAT AAG AGA CAG-3' and 5'-GTC TCG TGG GCT CGG AGA TGT GTA TAA GAG ACA G-3', respectively), as described by Kozich et al. (2013), and PCR amplifications were undertaken on an Eppendorf Mastercycler in a total volume of 50 μl using MyFi PCR Master Mix (Bioline Meridian Bioscience), 1 μl of each primer, and 1 μl of template eDNA with thermo-cycling conditions as specified by Pochon et al. (2020). PCRs included negative controls (1 per batch of reactions) using ddH_2O as template. Amplicons were purified and set at equimolar concentration (~2 ng μl^{-1}) using the SequalPrep™ Normalization plate kit (Applied Biosystems™). All aforementioned steps were performed in separate sterile rooms dedicated to these steps, with sequential workflow to ensure no cross-contamination. The PCR set-up and template addition were undertaken in laminar flow cabinets with HEPA filtration, and aerosol barrier tips (Axygen) were used throughout. Libraries were sent to Auckland Genomics for indexing and paired-end sequenced (2 × 250 bp) on a MiSeq™ platform. Sequence data can be retrieved from NCBI under project number PRJNA838716.

2.3.2. Bioinformatic analysis

Fastq files were demultiplexed and primers removed using 'cutadapt' (version 2.6; Martin et al. 2021).

Sequences were then truncated at 226 and 220 bp on the 3′ end to remove the lower-quality section, and quality filtered, denoised, paired-end merged, and chimera-filtered with the 'DADA2' R program (version 1.14; Callahan et al. 2016). Quality filtering and denoising were performed using the default parameters, merged using a perfect minimum overlap of 10 bp, and chimeras were removed using the consensus method. Amplicon sequence variants (ASVs) were taxonomically assigned using the RDP Naïve Bayesian Classifier algorithm (Wang et al. 2007) implemented in 'DADA2' and using the SILVA ribosomal RNA gene database (version 132; Quast et al. 2013). Sequences found in negative controls (i.e. DNA extraction, PCR, indexing and sequencing blanks) were identified and removed from downstream analysis. Sequences that were classified as chloroplast, that remained unclassified at the kingdom level, or were identified as non-bacterial, were discarded. Additionally, rare ASVs (less than 2 reads within at least 3 samples) were removed from the data set. Sequencing depth per sample was visualized with the 'rarecurve' function of the 'vegan' R package (Oksanen et al. 2022; Fig. S1 in the Supplement at www.int-res.com/articles/suppl/q017p001_supp.pdf), and samples with less than 2400 reads were discarded, to ensure that samples used in downstream analyses had sufficient sequencing depth to recover most of the diversity (Fig. S1). Finally, a phylogenetic tree of the ASVs was made in Qiime2 (version 2020.06; Bokulich et al. 2018) by first aligning sequences with 'mafft' (Katoh & Standley 2013), masking high ambiguity regions with the 'mask' function, creating a tree with 'fasttree' (Price et al. 2010), and rooting the tree with the 'midpoint-root' function.

Microbial compositions within and between samples were contrasted based on weighted-unifrac (Lozupone & Knight 2005) distance ordinations using permutational multivariate analysis of variance (PERMANOVA) procedures including pairwise contrasts within the 'adonis' function in the 'vegan' package in R.

2.4. Particle dispersal simulations

2.4.1. Resuspension in a turbulent environment

We constructed a simplified model of fecal particle disintegration in a turbulent environment. Initially, the sinking velocity follows the distribution of Bannister et al. (2016). After some time, particles are assumed to break into smaller pieces of equal size and the sinking velocity is assumed to scale with the diameter squared (i.e. Stokes' law). The breakup process stops when the particle size reaches a lower limit. More specifically, we set:

$$w_n(t) = w_n(0)\frac{S(t)}{S(0)} \quad (1)$$

where $w_n(t)$ is the sinking velocity of particle n after some time t and $S(t)$ is the mean cross-sectional surface area of the particles at time t, as measured by the image analysis procedure.

Existing experimental data do not give size-dependent values for the critical shear stress required for fecal particle resuspension (Cromey et al. 2002, Law et al. 2016, Carvajalino-Fernández et al. 2020b). We chose instead to model this relationship using the Rouse number:

$$P = \frac{w}{\kappa}\cdot\sqrt{\frac{\rho}{\tau}} \quad (2)$$

where w is the sinking velocity, $\kappa = 0.41$ is the von Karman constant, τ is the shear stress, and ρ is the fluid density (Lynch et al. 2014). When $P > 1$, the sinking effect is stronger than the turbulent upward mixing and the particle will be pinned against the bottom; horizontal motion during flight will be brief and small. Therefore, P must be <1 for fecal particles to be resuspended, giving a critical shear stress of:

$$\tau_c = \frac{\rho w^2}{\kappa^2} \quad (3)$$

2.4.2. Case study: Frøya Archipelago

A high-resolution hydrodynamic model was set up for a high-intensity Norwegian fish farming area, the Frøya Archipelago (63.6° N, 8.6° E). This is a dynamic, exposed coastal location consisting of 3 main islands and many smaller islets and skerries. Fish farms in this region are often located at relatively shallow depths, usually at 20–50 m. We used the Regional Ocean Modeling System (ROMS, Shchepetkin & McWilliams 2005, Haidvogel et al. 2008) with a 3-level 1-way nesting structure to model ocean currents and vertical turbulent mixing. The outermost nesting level is the NorKyst model system (Asplin et al. 2020), which has a horizontal resolution of 800 m. The intermediate level has a horizontal resolution of 160 m, while the innermost region covers an area of 21 km × 28 km with a horizontal resolution of 32 m × 32 m. All nesting models have 35 terrain-following vertical levels. The simulation period is 1 February 2015 to 12 August 2016. Details about the model and the nesting method are described by Carvajalino-Fernández et al. (2020b), who used a similar 2-level nesting structure.

The innermost nesting region of the hydrodynamic model contained 14 salmon farm locations that were active during the simulation period. The particle transport model Ladim (Ådlandsvik & Sundby 1994; https://github.com/bjornaa/ladim) was used to model fecal dispersal from each location. The breakup process and subsequent resuspension was implemented as a Ladim plugin (https://github.com/pnsaevik/ladim_plugins, version 1.2.1). Size and position of individual farm cages were taken from aerial photographs. This was available for all locations except the outermost one, where cages were placed manually in a plausible configuration. Fecal output was assumed to be 20% of the feed usage, in accordance with Cubillo et al. (2016). Excess feed was not included in the simulation. Actual feeding data from individual farms were used as model input, with peak production occurring around March 2016. In the simulation, 1 computational particle represented 1 kg of particulate organic matter (POM).

3. RESULTS

3.1. Biological and chemical state of sediments in chambers

3.1.1. Geochemistry

Natural chamber sediments were in an oxic state (Hargrave et al. 2008) with an overall average oxidative redox potential (ORP) of 106 mV with very low between-chamber variation (average range: 95–116 mV, Fig. 2C). Total free sulfide (S^{2-}_{UV}) concentrations were also consistently low and indicative of natural oxic sediments (Hargrave et al. 2008), with chamber averages ranging between 45 and 217 µM and an overall average of 90.6 µM (Fig. 2A). By contrast, the Impacted sediments were hypoxic-B or anoxic, with average ORP values between −108 and −302 mV and an overall average of −191 mV (Hargrave et al. 2008), or in the range of 'bad' to 'very bad' (standard 2 or 3) according to Fig. D.1 of the Norwegian standard (NS 9410:2016, Standards Norway 2016). Average S^{2-}_{UV} on the impacted sediments was 2771 µM and ranged between 356 and 7387 µM across the chambers (Fig. 2A), and accordingly, most chambers were considered 'anoxic' and indicative of a 'bad' ecological quality (Cranford et al. 2020). Highly significant differences were observed between the Impacted and Natural sediment for all 3 geochemical properties, and within each sediment type (i.e. Natural or Impacted), the chambers that had feces added were considered similar to those that did not.

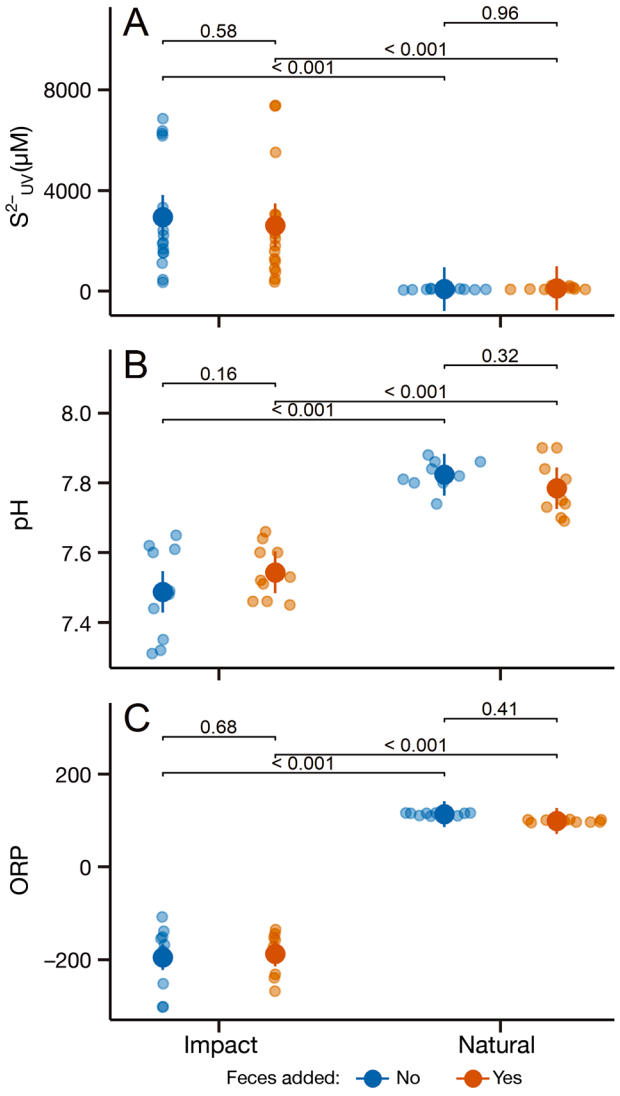

Fig. 2. Marginal-mean values (large dots) and upper and lower confidence intervals for (A) total free sulfide (TFS) concentrations, (B) pH, and (C) oxidative redox potential (ORP) of sediments in each chamber at the conclusion of the experiment. Modeled effects (p-values) for pair groups from associated linear mixed effect models (treating chamber replicate as a random factor) indicated n (per chamber) = 2 for pH and ORP, and 3 for TFS. Vertical error bars represent 95% confidence interval

3.1.2. Macrofauna

The natural sediment chambers each contained between 12 and 39 individual fauna representing 8–17 different taxa (Fig. 3A,B). The composition of the fauna was relatively diverse and mostly indicative of natural sediment, evidenced by AMBI scores between 1.5 and 3.1 (indicative of 'unpolluted' or 'slightly polluted' sediments; Borja et al. 2000), and

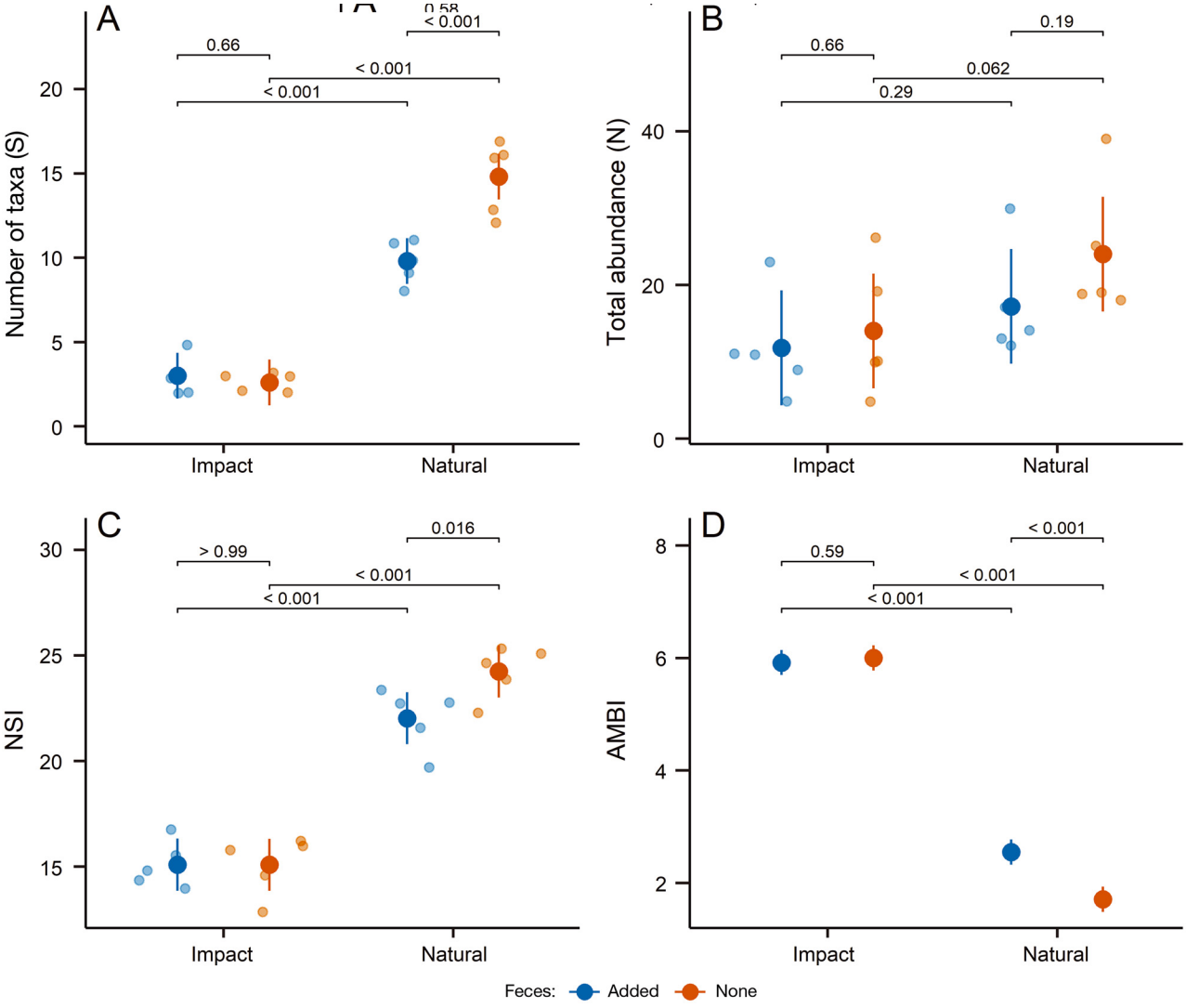

Fig. 3. Mean values (large dots) and upper and lower confidence intervals (vertical lines) for macrofauna statistics: (A) number of taxa (S), (B) total abundance (N), (C) Norwegian Sensitivity Index (NSI), and (D) AZTI's marine biotic index (AMBI) from each chamber at the conclusion of the experiment (n = 1 per chamber). Modeled effects (p-values) are indicated for pair groups from the associated linear model. Vertical error bars represent 95% confidence intervals

the NSI scores were correspondingly relatively high (19.6–25.4, Fig. 3D,C). By contrast, the impacted sediments had very low species richness (2–5 taxa per chamber) but a comparable total abundance (5–26 individuals per chamber, Fig. 3A,B). The fauna was strongly dominated by 2 species, the polychaete *Capitella capitata* and the crustacean *Nebalia bipes*, which are both hardy, opportunistic species found in association with decomposing organic waste. During the trials, another common opportunistic species, *Ophryotrocha* sp., was observed feeding on the pellets, but it was not found in the samples which were sieved at the end of the experiment. It was assumed that these organisms had either perished due to exhaustion of the food source and/or the advancement of anoxia within the highly enriched chambers. Accordingly, the AMBI scores were consistently high, ranging between 5.6 and 6.0, indicating a 'heavily polluted' state, and the NSI scores were low (Fig. 3D,C). For all variables, the Natural sediments were highly significantly different from the Impacted sediments. Within the Impacted sediments, the chambers with feces added were statistically similar to those without added feces, whereas for the Natural sediments, feces-added sediments were considered significantly different from non-added sediments for S (number of taxa), NSI, and AMBI at the conclusion of the experiment.

3.1.3. Microbial composition

A total of 7 988 739 reads (mean: 76 815 per sample) were sequenced. After performing quality filtering, denoising, merging, and removing chimeras, a total of 4 987 608 reads (mean: 47 958 per sample) remained. Removal of sequences found in the blanks reduced the read count by 2.9% and resulted in the loss of 0.12% (73) ASVs. Discarding non-bacterial sequences and those either assigned to chloroplast or unidentified at the kingdom level resulted in the loss of 14.5% of the reads. Finally, the removal of rare ASVs (those with fewer than 2 reads in at least 3 samples) led to a mean read count of 39 689 per sample, with all samples reaching near complete sequence coverage (Fig. S1).

At the ASV level, the microbial communities present in the 2 sediment types (Natural and Impacted) at the start of the experiment were strongly significantly different (pairwise.adonis p_{adj} = 0.0001, Fig. 4A; Table S1). Both the Natural and the Impacted sediments were considered significantly ($p < 0.01$) different from the feces and seawater, and mildly significantly different ($p < 0.05$) from the food. When grouped at the genus level, the 2 sediment types shared 66 taxa, with 52 taxa being distinct to Natural sediments and 61 distinct to Impacted sediments (Fig. 4B). The impacted sediments generally shared greater similarity with the feces, while Natural sediments were more similar to seawater (Fig. 4).

3.2. Particle breakup and decay

3.2.1. Natural sediment

Feces clumps on unimpacted Natural sediments remained largely cohesive and intact for the first 60 h, during which time they could be dislodged from the sediment with the controlled disturbance. The main breakup phase began after approximately 90 h, when the mean number of particles began steadily increasing and individual particle size began steadily decreasing (Fig. 5A). Over this period, the total area occupied by the particles remained relatively constant. There were 2 main breakup phases, between 90 and 110 h, and between 160 and 200 h, with a stable period in between (Table 1). During the breakup phases, the average individual particle area reduced from approximately 0.25 to 0.08 cm^2, which equates to a disaggregation rate of approximately 0.25 $cm^2\ d^{-1}$.

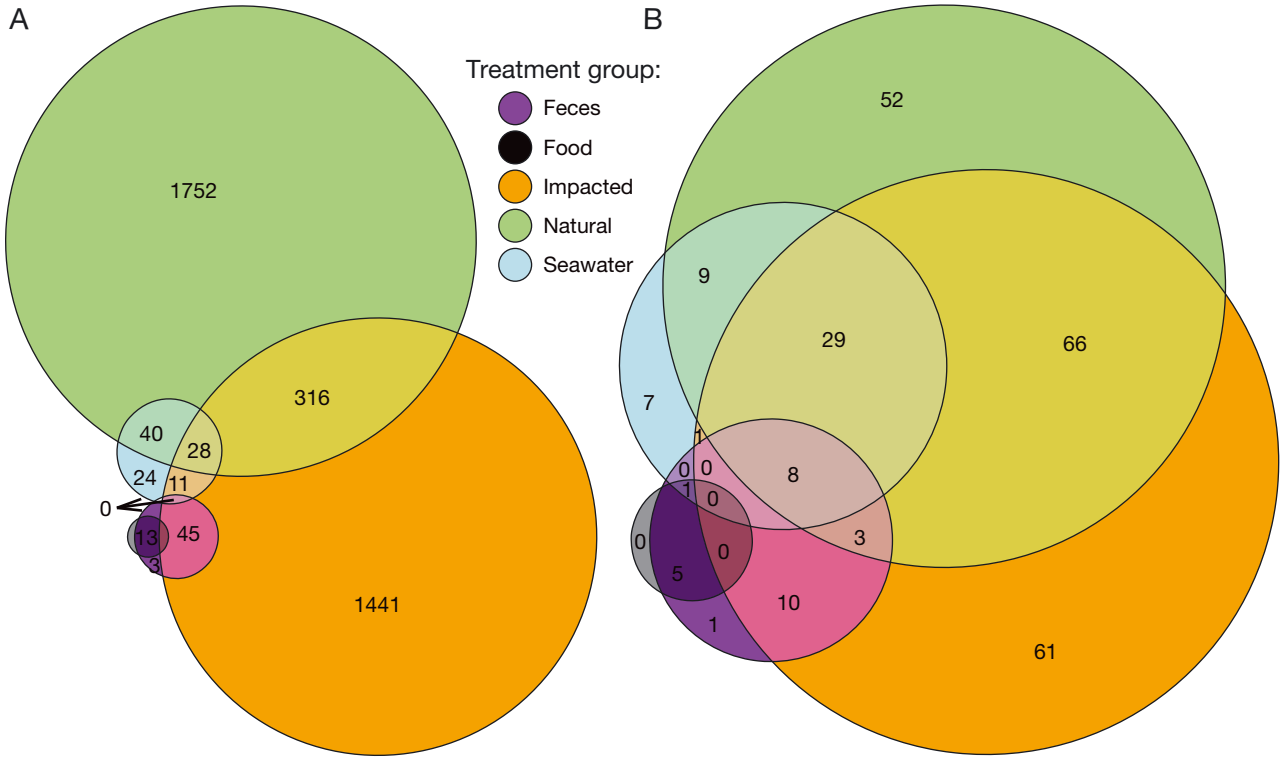

Fig. 4. Proportionately sized circles showing the degree of commonality between microbial taxa at the start of the experiment for the 2 sediment types (Impacted and Natural), feces, feed fed to the fish (Food), and the seawater flowing through the chambers, for (A) amplicon sequence variant (ASV)-level data and (B) genus-level grouping, all transformed to presence/absence

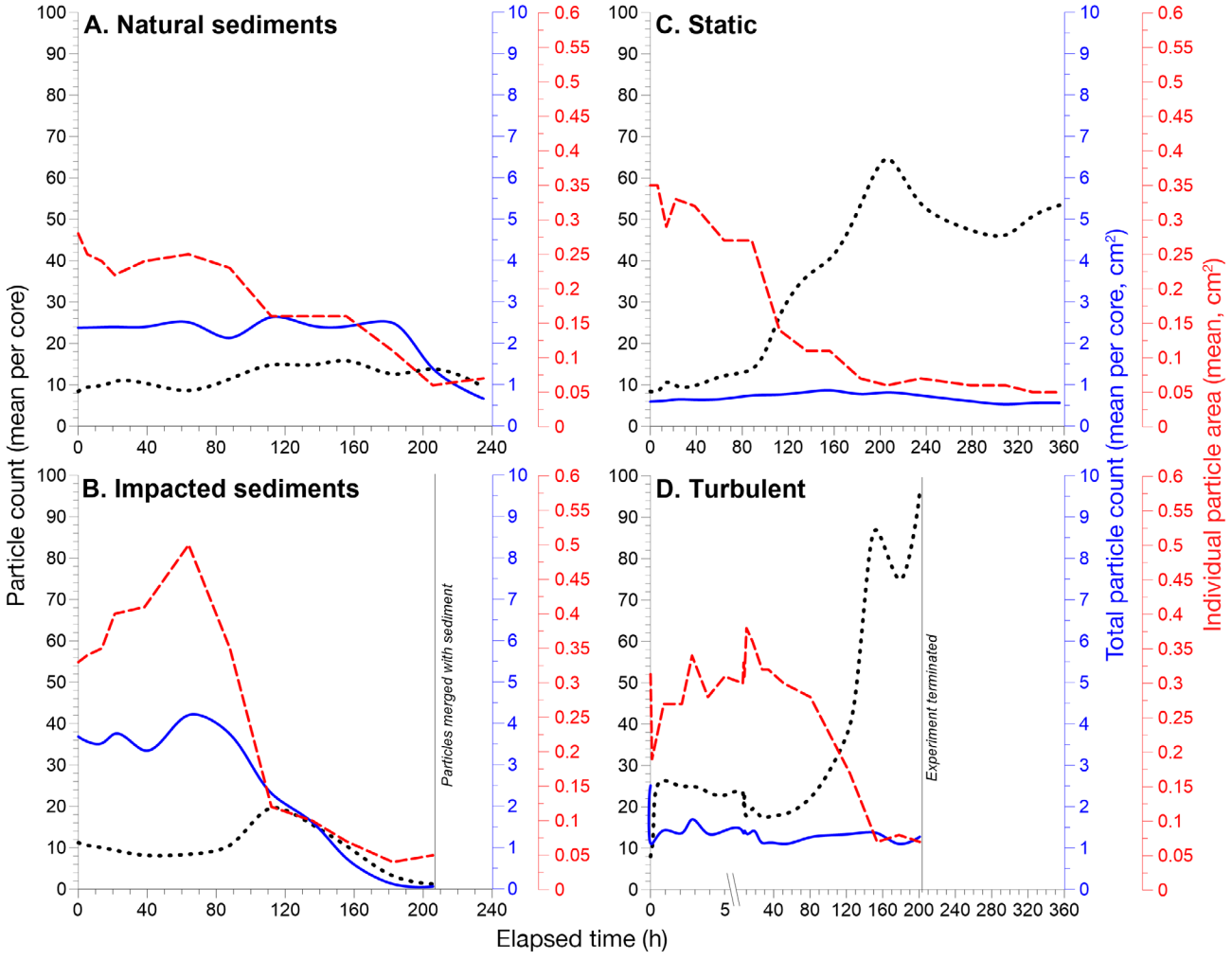

Fig. 5. Summary of mean particle count (black dotted line), mean individual particle size (red dashed line), and mean total area of particles (blue solid line) on (A) Natural and (B) Impacted sediments, and in (C) Static and (D) Turbulent chambers over the course of the experiment

Table 1. Summary of particle size, breakup process, and time to effective disappearance. Start and End of main breakup phase are indicated by sustained decrease in particle size and corresponding (inverse) increase in particle number

Treatment	Start dimensions		Peak particle abundance			Main breakup phase				End points		
	Count #	Size (cm^2)	Time (h)	Count #	Size (cm^2)	Start (h)	End (h)	Duration (h)	End size (cm^2)	Mean size <20% (h)	Count <20% (h)	Total area <20% (h)
Natural	9	0.3	160	16	0.32	90	200	110	0.1	210	>240	>240
Impacted	10	0.36	115	20	0.23	65	110	45	0.12	160	195	155
Static	9	0.36	210	65	0.07	90	190	100	0.07	180	>360	>360
Turbulent	8	0.32 (0.19)[a]	200	96	0.07	10[b]	150	140	0.06	150	>200	>200

[a]Size at start based on average size at time of first measurement in non-turbulent chambers; bracketed value is size at T1 after initial disaggregation
[b]Initial breakup phase from 8 to 27 particles occurred almost instantaneously, prior to this subsequent breakup phase

At 110 h, the particles were still clearly visible on the sediment in a partially integrated broken-down state with low vertical relief, while some were still visible at the end of the experiment after 240 h (Fig. 6). Mean individual particle size achieved 20% of the start size after 210 h, but the <20% threshold was not reached within the experimental period (240 h) for total count and area.

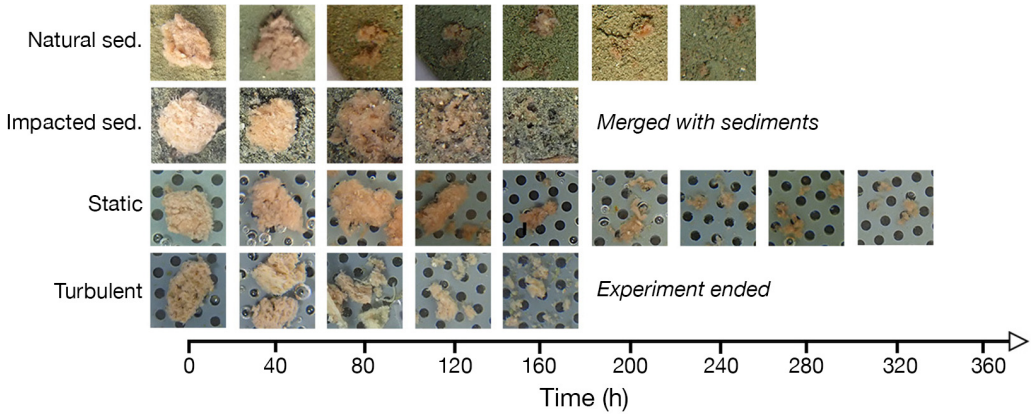

Fig. 6. Indicative fecal particles for each of the 4 treatments at 0, 40, 80, 120, 160, 200, 240, 280, 320, and 360 h over the course of the experiment

3.2.2. Impacted sediment

During the first 65 h, particles on Impacted sediment decreased slightly in number, while at the same time, individual particle area increased sharply, due to some of the smallest particles disappearing, while the main large particles were visibly disintegrating and spread out on the sediment surface. After 90 h, mean individual particle area declined rapidly, total area began to decline, and mean particle count increased (Fig. 5B). During the main individual particle breakup phase, the approximate disaggregation rate was 0.5 $cm^2\ d^{-1}$. Notably, within 12 h of the experiment commencing, infaunal polychaetes were observed emerging from the sediment and moving through the fecal particles, creating tunnels and breaking down the feces structure (Fig. 7). After 24–48 h, the pellets were partially bound to sediments but disaggregated easily on disturbance, with small loose fragments easily mobilized. This breakup phase is reflected in the increased particle count between 80 and 110 h. After approximately 100 h, the particles were mostly reduced to a patchy, flaky mass on the sediment, were semi-integrated, and could not be easily dislodged with water movement (Fig. 6). After this time, individual size, total area, and count reduced consistently, achieving near zero values

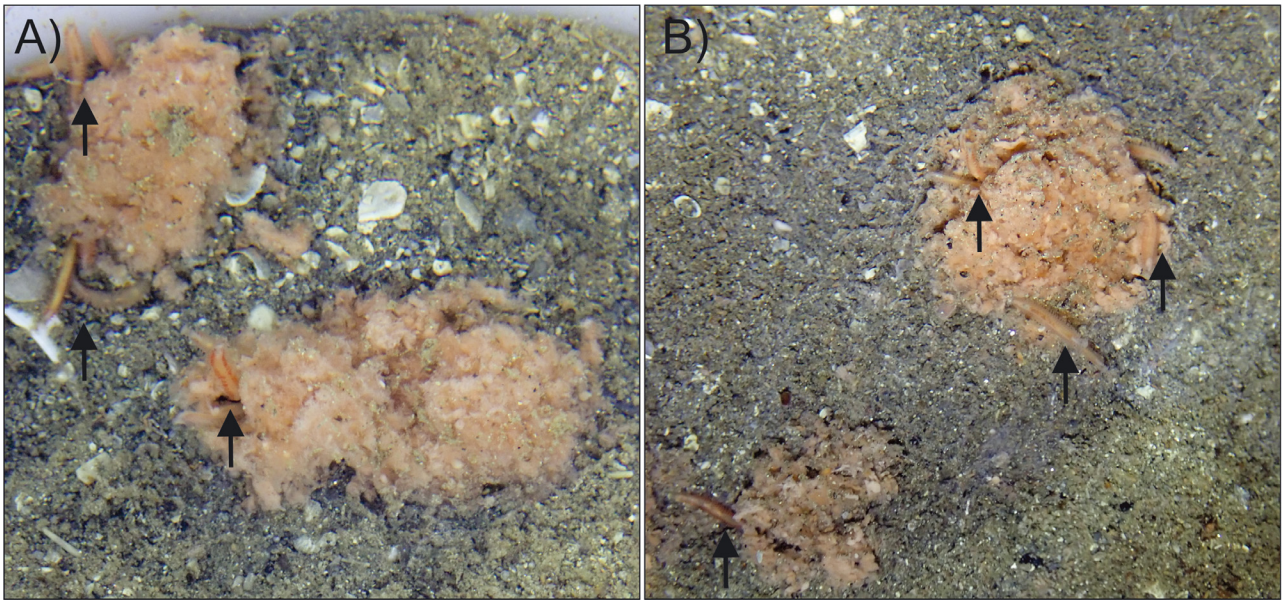

Fig. 7. (A,B) Partially degraded fecal pellets on impacted sediment with opportunistic polychaetes (*Ophryotrocha* sp. and *Capitella* sp.) on and around the pellets (indicated by black arrows), accelerating decomposition

after 180 h (i.e. breaking up and decaying or being consumed). Total particle count and total area were reduced to <20% of the start points after 195 and 155 h, respectively (Table 1). This was the only treatment in which this was achieved.

3.2.3. Static chambers

Between 0 and 90 h, the particles in the Static chambers remained in a relatively stable state, decreasing slightly in individual size and increasing slightly in count and total area (Fig. 5C). After approximately 90 h, the average size decreased progressively from 0.27 to 0.07 cm^2 by 190 h and the corresponding disaggregation rate was 0.27 cm^2 d^{-1} (Table 1). Over the same period, the mean number of particles increased from 14 to 66, but the mean total particle area remained relatively unchanged (i.e. gradually breaking apart but not decaying). Particles were easily dislodged upon disturbance throughout. From 180 h, the mean size and number of particles remained relatively stable, and approximately 53 particles of 0.05 cm^2 were still visible at the end of the experiment (after 360 h).

3.2.4. Turbulent chambers

In the Turbulent chambers, there was an abrupt, nearly instant increase in mean particle number (from 9 to 27) as fragments separated from the initial aggregate particles, and a corresponding decrease in mean particle size as soon as the particles were introduced to the turbulent water (Fig. 5D). This initial breakup occurred before the first image was taken. However, at the start, particle sizes were similar to those that were used in the other treatments, which means an instantaneous disaggregation from a mean size of 0.32 to 0.19 cm^2. During the ensuing 10 h, some reaggregation occurred as the average size gradually increased to 0.38 cm^2 (Fig. 5D). Between 10 and 80 h, individual particle size decreased and total count increased steadily. After 80 h, a stronger linear breakup phase occurred as mean particle size decreased more rapidly and the number of particles increased accordingly. Particle breakup was largely complete after 150 h (reaching 20% of the start threshold), at which point the 10 initial 0.3 cm^2 fecal particles had divided in to approximately 88 smaller (0.05–0.1 cm^2) particles (Fig. 5D, Table 1). Numerous small particles were still visible at the conclusion of the experiment, and the total area (and approximation for mass) also remained relatively unchanged. The Turbulent experiment was terminated after 200 h because the size of the particles had reduced to the point at which they could pass through the gaps in the perforated flow diffuser which was retaining them in the turbulent water.

3.3. Microbial inoculation of sediments

At the ASV level, the Natural sediment that had feces added was the only treatment that demonstrated an appreciable shift towards the microbial composition of feces and feed during the experiment (Fig. 8A). Feed and feces had 14 ASVs in common, one of which was found in the Natural sediments at the conclusion of the experiment. An additional 5 ASVs were common to the feces and in the After sample from the sediment that had feces added, but were not found in the Before samples from the same chambers, nor in the chambers that did not have feces added. These bacteria included 2 *Proteobacteria* ASVs (*Kiloniellaceae* and *Cellvibrionaceae*), 2 *Bacteroidota* (both from the family *Flavobacteriaceae*), a *Firmicutes* (family *Streptococcaceae*), and 1 ASV from the order *Desulfobacterales*.

Similar trends were evident in the genus-level data, with a small but notable migration of the Natural sediment with the feces added, demonstrating an increased number of shared taxa at the conclusion of the experiment (Fig. 8C). For the Impacted sediments, both types of chambers (feces added and not added) had slightly fewer taxa in common with feces and feed at the conclusion of the experiment, along with the addition of some new genera that were not found in any of the other possible sources (Fig. 8D).

A PERMANOVA model comparing the ASV composition (weighted unifrac ordination) in the Natural sediments showed a highly significant interaction between the effect of feces addition (added versus not added, $F_{1,36}$ = 2.5841, p = 0.0001) and time (before versus after, $F_{1,36}$ = 2.9663, p = 0.0001, Table S2A). Pairwise contrasts of the model (Table S3A) showed that this interaction was due mainly due to the influence of feces being added to the sediments. At the conclusion of the experiment, the Natural chambers that had feces added were significantly different from both the chambers with and without feces added at the start of the experiment (F = 0.0017, p = 0.0018 and F = 0.0022, p < 0.0001, respectively; Table S3A), and also different from the Natural sediments that did not have feces added at the end of the experiment (F = 0.0015, p = 0.0049; Table S3A).

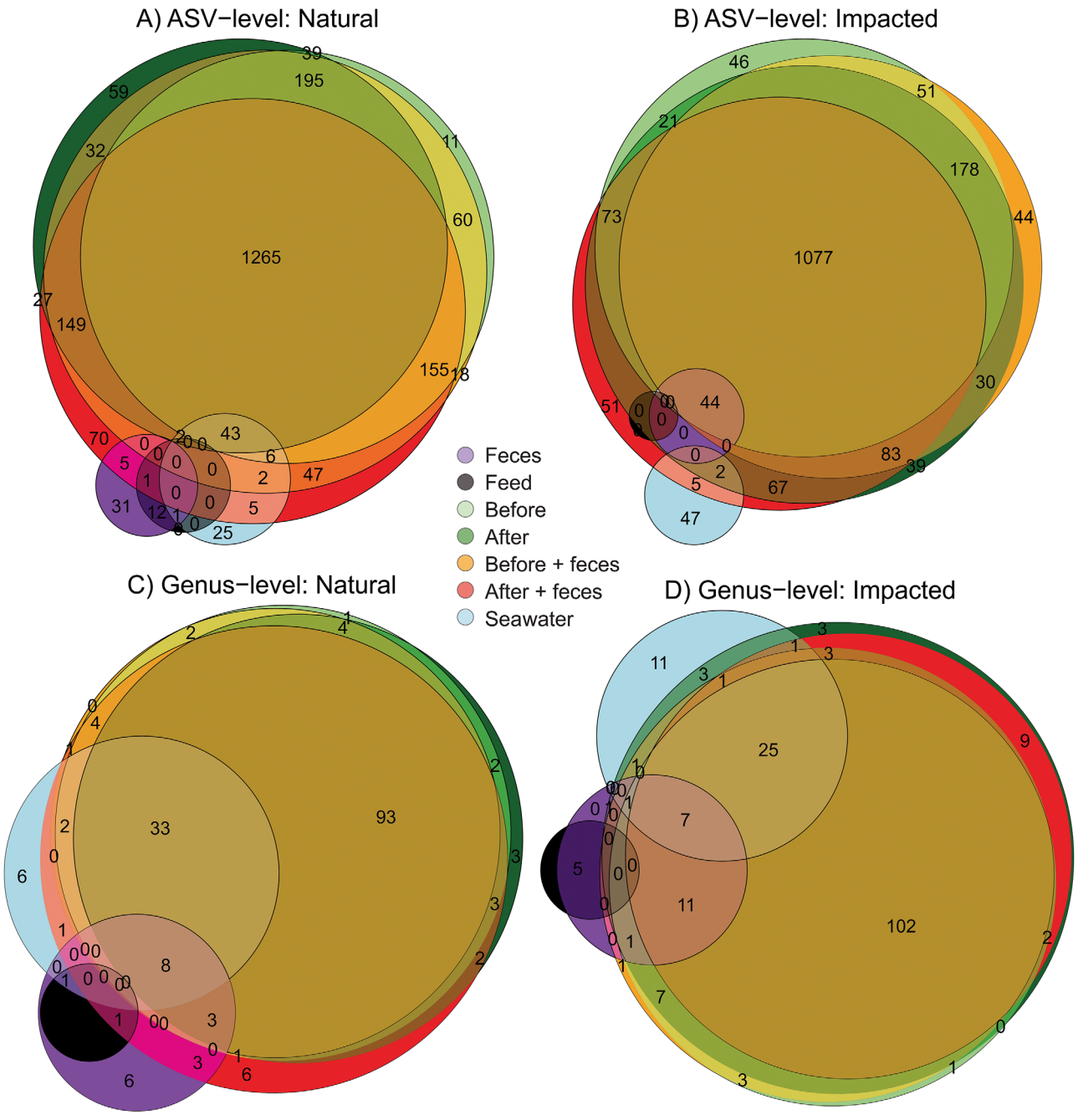

Fig. 8. Proportionately sized circles showing the degree of commonality between microbial taxa for the 2 sediment types (Impacted and Natural) with and without feces added, before and after the experiment, and in relation to the feces, food fed to the source fish (Feed), and the water supplied to the chambers. (A,B) Amplicon sequence variant (ASV)-level data, all transformed to presence/absence; (C,D) genus-level grouping

For the Impacted sediments, the Time × Feces addition interaction was only mildly significant ($p = 0.035$; Table S2B), while the fixed factors were both highly significant. The differences were all due to the factor Time, i.e. the After sediments were different from the Before sediments (Table S3B).

3.4. Implications for particle dispersal modeling

3.4.1. Resuspension in turbulent environments

Results from the Turbulent trials show that the mean particle size decreased to 65% of the original value al-

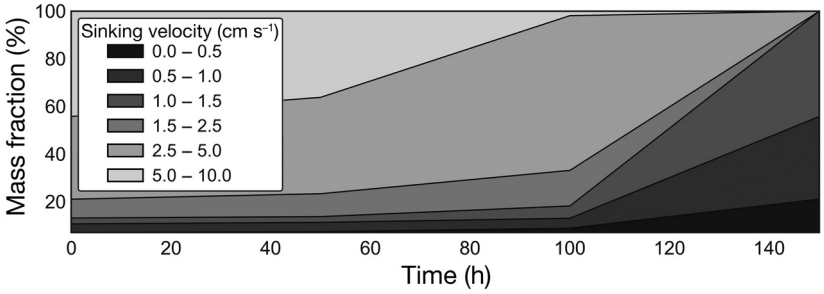

Fig. 9. Evolution in sinking velocity distribution for particles in a turbulent environment

most immediately, then after some reaggregation, disaggregated progressively to approximately 15% at 150 h. After 200 h, particle size fell below the experimental size limit. When these breakup phases and associated particle sizes were applied in conjunction with the initial distribution of sinking velocities from Bannister et al. (2016), a major distribution shift with time was evident (Fig. 9). Before breakup, 66% of the particles sank faster than 5 cm s^{-1} and 85% of the particles sank faster than 2.5 cm s^{-1}. Almost no particles sank faster than 5 cm s^{-1} after 100 h, and all particles sank slower than 2.5 cm s^{-1} after 150 h. As sinking velocity was linked to critical shear stress in our model, smaller sinking velocities mean that more material is resuspended and transported further away.

3.4.2. Case study: Frøya Archipelago

The ocean currents at the Frøya Archipelago are strongly influenced by the Norwegian Coastal Current, which originates from the Baltic Sea and follows the entire Norwegian coast. Tides and wind-driven currents interact with topographic features to produce a highly dynamic flow pattern. The median modeled vertical turbulence coefficient 1 m above the sea floor at the aquaculture locations was 9.2 × 10^{-4} m^2 s^{-1} throughout the simulation period. The lower quartile was 8.5 × 10^{-5} m^2 s^{-1} and the upper quartile was 3.3 × 10^{-3} m^2 s^{-1}. There is a significant seasonal pattern, with higher values of vertical turbulence in the winter months compared to the summer months (see Fig. S2). Of the 14 sites, 13 are located at depths ranging from 20 to 50 m. When particle dispersal was simulated with no breakup physics, only 5% of the fecal material settled further than 1 km from the release point. When breakup was accounted for, 15% of the material settled further away than 1 km, and 2% of the material spread more than 10 km away. In several areas, the waste footprints were continuous between farm localities (Fig. 10).

4. DISCUSSION

4.1. Particle breakdown and implications for models

Particle decomposition was strongly affected by sediment type, whereby particles placed on impacted sediments were broken down and metabolized appreciably faster than those on 'natural' (unimpacted) sediments. Additionally, breakdown on both sediment types was faster than for particles on an inert substrate in similarly static water. Results suggest that particles

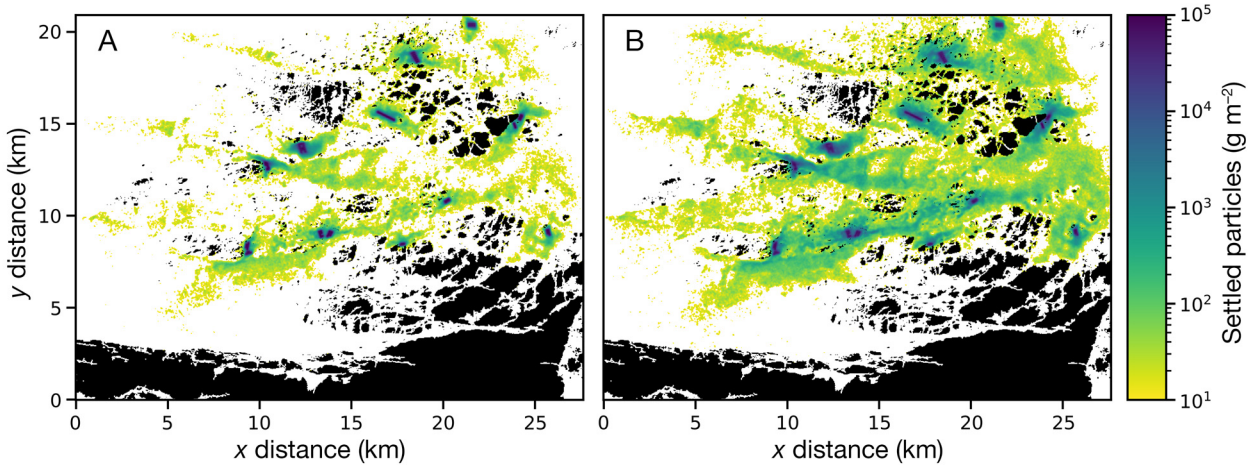

Fig. 10. Model simulations for dispersion and settlement of particulate waste from salmon farms in the Frøya Archipelago using the traditional approach (A) without considering particle breakup, and (B) with particle breakup according to the particle behavior identified in the turbulent experimental chambers

that land on natural sediments remain intact and generally unbound for approximately 90 h before progressively breaking down into smaller particles of approximately 0.1 cm^2 over the next 40 h. Particles on natural sediments were metabolized ('removed from the system') and integrated into sediment after approximately 240 h. Particles landing on highly organically enriched 'impacted' sediment remained mostly intact for 85–90 h, but thereafter breakdown and integration into the sediment occurred relatively rapidly. Sediment integration was near-complete after approximately 100–120 h, and the introduced particles were visually metabolized, and therefore removed from the system (in a physical sense), after 160–195 h. Macrofaunal activity (in this case, primarily *Ophyrotrocha* sp., but also *Capitella* sp.) played a visually conspicuous role attaching to and breaking down the waste, which is not unusual, as both species are effective waste decomposers and enrichment tolerant (Kinoshita et al. 2008, Svensson et al. 2023). This biological process may in fact explain the phenomenon where models for dispersive sites predict 100% dispersion of particles out of the model grid, yet benthic effects are observed (Keeley et al. 2013b, Fox et al. 2023), i.e. the fauna trapping particles and thereby integrating carbon into the sediments is the enrichment mechanism. The contrast between natural and impacted sediment decomposition rates was presumably also a function of the relatively distinct microbial communities that are consistently associated with enriched sediments (Frühe et al. 2021, Keeley et al. 2021). Such alterations are linked to metabolic functions, in particular, the anerobic bacteria and associated sulfate reduction pathways that are characteristic of faunated organically enriched sediments with strongly elevated microbial abundance and correspondingly, metabolic capacity for organic matter (Kristensen & Holmer 2001, La Rosa et al. 2001, Vezzulli et al. 2002, Valdemarsen et al. 2010).

Having visual confirmation of the breakdown process and an indication of approximate timelines provides much needed insight into how to treat particle fate in dispersion models. The time at which a particle becomes part of the seabed and therefore no longer available for resuspension, also termed 'consolidation time' (Cromey et al. 2002), is important because it determines the particles' availability for subsequent transportation within the model grid, and therefore the potential spatial extent of influence. To date, in the absence of real-world observations, this parameter has been estimated and generalized for all environments. Earlier models have used 4 d (96 h), based on numerical sensitivity analyses (Cromey et al. 2002), while others have employed a simple exponential decay function to mimic breakdown via microbial pathways (e.g. Elvines et al. 2024). The results of our study are partially congruent with the original estimate by Cromey et al. (2002), i.e. fecal 'particles' in static water maintained their physical properties for the first 90 h. However, on sediments, the propensity for resuspension differed strongly in accordance with the benthic enrichment state. On impacted sediments, the breakdown and decomposition to smaller flakes started at 65 h and peak abundance occurred at 115 h. While the propensity for resuspension and retransportation was higher during this period, there was also a biological factor which served to negate resuspendability on impacted sediments, i.e. many of the particles appeared partially bound after only 24–48 h due to the activity of the macrofauna. In some cases, several polychaetes attached to the particle within hours of it being introduced, in effect attaching it to the sediment before the fauna proceeded to move through and around the particle, metabolizing the constituents (Fig. 7). In contrast, particles on natural sediments tended to break down into numerous, smaller fractions that were readily resuspended and persisted in that form for an additional 100+ h. This study therefore suggests that consolidation times differ in accordance with benthic enrichment state, and that a suitable consolidation time for highly impacted sediments is between 48 and 160 h (dependent on macrofauna activity), and for natural sediments may be as high as 240+ h.

The breakup and formation of smaller particles in the Turbulent and Natural chambers has significant implications for critical erosion thresholds and settlement rates (Law et al. 2014) and therefore particle dispersal modeling. Depending on density, smaller particles are likely to be resuspended earlier and settle slower (Chen et al. 1999, Bannister et al. 2016), which will significantly extend the spatial range of the effects footprint, albeit in a more dilute form. There are 2 main opposing processes that control the size and shape of particles once in solution: aggregation (flocculation) and disaggregation. Flocculation of smaller particles into larger, faster-settling aggregates is a function of particle encounter rate (size and density), contact efficiency, and stickiness, and is opposed by disaggregation, primarily from turbulence-induced breakup (Hill 1996, Hill et al. 2013, Milligan & Law 2013). During this experiment, very little aggregation was observed apart from in the Turbulent chambers, where mean particle size gradually increased in the short-term (0–10 h), before progressing to a disintegration phase, achieving a mean size of 0.27 cm^2

after approximately 80 h and 0.07 cm^2 after 150 h. The 80–90 h mark seems to be an important particle 'age' at which the integrity of the particles weakens (presumably from microbial activity on the protein structures) and more readily disaggregated into smaller 'base constituent' particles, as was evident in both the Static and Natural sediment chambers. Therefore, for particles entering turbulent waters, characteristic of high-current sites, there are 2 theoretical stages in particle size dynamics and associated settling velocity and distribution trajectories: the first is a near-instant disaggregation followed by reaggregation to a similar size within 10 h, which would therefore have limited impact in a model, which typically simulates much longer periods. The second, more important phase is the initial disaggregation that occurred between 10 and 80 h of soak time, followed by a phase of more rapid breakup until 160 h. To demonstrate the impact of including these processes, the size-specific sinking rates were estimated based on an established particle diameter to settling velocity relationship ($y = 0.214 + 4.07x - 1.40x^2$; where y = settling velocity [m s^{-1}] and x = particle area [cm^2]; Law et al. 2014). On this basis, the particles that were used to initiate the experiment (ca. 0.35 cm^2) would sink at ~1.5 m s^{-1}, whereas after the initial break up, the finer 0.07 m^2 particles would sink at ~0.5 m s^{-1}. Therefore, theoretically, at a 50 m deep site, these 2 particle sizes would take approximately 34 and 101 s, respectively, to fall to the seabed, meaning that the finest particles would be subjected to horizontal transportation forces for 3 times the duration.

Particle size and, by proxy, sinking velocity also relate to critical shear stress, which defines the propensity for resuspension and ongoing transportation, roughly according to the Rouse number (Lynch et al. 2014). Hence, particle breakup affects particle dispersion in multiple ways. Having the ability to model these processes is obviously most important for sites with strong hydrodynamics. Our simulation of the highly dynamic and salmon farm-rich Frøya region in central Norway (Fig. 10) exemplifies this point, whereby the model predicts appreciably higher fluxes (g m^{-2}) of waste particles at distances beyond 1 km from the source. In effect, a much smaller portion of the waste is predicted to settle out directly under the farms and is instead transported further afield before settling. The result is that the depositional footprints from the farms are predicted to be generally less distinct but collectively influence a larger area, with a higher degree of interconnectedness between farms. This finding has important implications for farm positioning and scope for overlapping effects.

Although the predictions for a larger waste influence field are seemingly at odds with historical literature that describes discernable effects dissipating within 50–200 m from a farm (Brooks et al. 2002, Giles 2008, Borja et al. 2009), this is not necessarily the case. Other studies (some of which are from the same study region) have traced waste and observed some effects out to and beyond 1 km (Sara et al. 2004, Woodcock et al. 2018, Keeley et al. 2019). Additionally, it is apparent that well-flushed dispersive sites can both assimilate waste at a higher rate and recover more rapidly for a variety of physical, chemical, and biological reasons (Keeley et al. 2019, 2020). Therefore, although a greater portion of the waste may be reaching far-field locations, the carbon flux may be within the assimilative capacity of the receiving environment (Bravo & Grant 2018). There are also a number of factors that can induce benthic effects in the near-field, despite the particles being subject to strong and generally constant advection forces. Firstly, the near-field locations will still be subjected to a greater intensity of particles and the residence time on the seabed (in-between resuspension events) can be sufficient to impact the benthos (Keeley et al. 2013a, Fox et al. 2023). Secondly, there are some physical and biological factors that may be acting to trap or bind the particles, thereby limiting resuspension and further transportation. For example, coarse substrates are thought to provide refuges for particles (Carvajalino-Fernández et al. 2020a, Fox et al. 2023), larger physical features can also inhibit transportation (this is also an unresolved artifact of sediment traps), as was observed in the experiments, opportunistic benthic fauna can also trap particles preventing resuspension, and the formation of biological films can resist erosion (Droppo et al. 2007); all of these factors are poorly quantified and accounted for in dispersal models.

As a final word of caution, the model that has been applied here should still be viewed as a general approximation of the breakup process: real particles do not necessarily break into equisized pieces, and the breakup rate may be dependent on the initial particle size. Also, the shape of the particle fragments is not necessarily the same as the original particles, which affects sinking velocity. Even the density of the particles may change if the particles become more porous over time, and not least, it is well established that feces composition is affected by fish diet and associated gut health (e.g. Baeverfjord & Krogdahl 1996, Hu et al. 2016). Therefore, although this study contributes an advancement towards capturing the true complexity of particle dynamics for modeling

purposes and demonstrates the consequences for particle dispersal, further work is needed.

4.2. Microbial inoculation of the seabed

Results from this study suggested minor scope for microbial inoculation of the seabed through the introduction and subsequent decay of fish feces particles. The natural sediment inherited 5 ASVs from the feces that were added. Conversely, the impacted sediments changed in a manner that was more consistent with oxygenation and recovery during the experimental period from what was a highly enriched state and did not inherit any new ASVs that were common with the feces. Of the 5 potentially 'exogenous' ASVs that were seemingly transferred to the natural sediments, 2 are associated with organic enrichment processes (i.e. nitrate reduction for *Kiloniellaceae*, Wiese et al. 2009; and sulfate reduction and hydrogen sulfide production in the case of *Desulfobacterales*, Burow et al. 2014), 2 are broadly classified as heterotrophs, and the other (*Streptococcaceae*) is linked to animal symbionts and parasites (Vandamme et al. 1996). Although relatively minor in terms of overall composition, the possibility that the microbiome in sediments can be influenced by a relatively varied addition of waste from farmed fish fed extraneously sourced diets could have quite profound environmental implications. Firstly, even a small alteration to a community that has important central roles in benthic metabolism, sulfate and nitrogen reduction pathways, and benthic productivity generally (Paerl & Pinckney 1996) could be functionally important. That said, it is difficult to assess the scope for this impact due to limitations in our understanding of ASV-specific functions and aspects such as persistence in the natural environment once introduced. Secondly, in the case of sea-based fish farms, although the changes may be subtle, the potential area of influence could be relatively large; i.e. a 'footprint' of several hectares as demonstrated in Fig. 10 and reported elsewhere (Keeley et al. 2013b).

There was also evidence to suggest that the Natural sediments were slightly (but significantly) organically enriched from the introduction of only 3–5 fecal pellets per chamber (equivalent to a single flux event of 288–481 pellets m^{-2}). While the Impacted sediments were chemically and biologically similar at the end of the trials, the Natural sediments with feces added were found to have a statistically lower number of taxa and NSI score, and higher AMBI compared with the Natural sediments without feed added. All of these results are consistent with progression to an increased state of enrichment (Hargrave et al. 2008, Keeley et al. 2012). It should also be acknowledged that the geochemical state of the sediments in the chambers may not be directly indicative of the natural pre-sampling state. The disturbance during transfer from grab to chambers was likely associated with some mixing of oxic and anoxic layers, thereby exposing reduced compounds to oxygen and increasing oxygen demand and promoting metabolic activity. The extent to which this caused the chamber sediment to differ from the *in situ* state was not quantified but is likely to be small in comparison to the contrast between the impacted and non-impacted sediments.

The finding that some changes were observed with a one-off introduction of only a few pellets (4–5) per chamber suggests that a relatively persistent low-level flux of pellets has the potential to influence sediments even some distance from a farm. To give this broader context, at the outer (least intensive) extent of the waste footprint simulated in Fig. 10, the accumulated mass was 10 g m^{-2}, which equates to approximately 833 particles m^{-2} over the modeled period (558 d), which in turn equates to 39 particles per fortnight (the duration of this experiment); i.e. approximately an order of magnitude more than was used in the experiment. This was estimated by calculating the mass of a single particle based on the average measured particle area (~0.3 cm^2), treating that as a circle and calculating the corresponding spherical volume (~0.12 cm^3), and then using a published fecal particle density estimate (Bannister et al. 2016; 0.1 g cm^{-1}) to arrive at a mass of 0.012 g $pellet^{-1}$. Collectively, therefore, the findings of this study suggest that: (1) current dispersal models may underestimate the horizontal dispersion of waste, and (2) the biological and chemical burden associated with these introduced waste particles has the potential to influence both the microbial composition and enrichment status of sediments, even at relatively low levels of deposition. It is recommended that this assumption be further explored with an extended experiment with repeated introduction of pellets, followed by a recovery period. These are factors that should be considered in the design of environmental monitoring programs that have the goal of targeting transitional and outer limit of effects zones (e.g. Norwegian c-investigations, Standards Norway 2016). It is also prudent to consider incorporating methods capable of detecting small alterations to microbial communities in near- and far-field environments in future monitoring programs.

Data availability. Unprocessed sequences are accessible from the NCBI Sequence Read Archive (SRA) under project number PRJNA838716. Metadata for the samples are available in the tables in the Supplement.

Acknowledgements. The support and funding for this project was provided by the Norwegian Research Council under projects: #267829 – 'SUSTAINable AQUAculture in the North: identifying thresholds, indicators and tools for future growth', and #320076 - AQUAed: 'On-site monitoring of aquaculture impact on the environment by open-source nanopore eDNA analyses'. We greatly appreciate Thor Arne Hangstad from Akvaplan NIVA, Tromsø, for kindly providing the wet lab facilities to undertake the experiments. We also thank the Havbruksstasjon in Tromsø for providing access to, and assisting with, extracting fresh salmon feces from cultured fish.

LITERATURE CITED

Adams TP, Black K, Black K, Carpenter T, Hughes A, Reinardy HC, Weeks RJ (2020) Parameterising resuspension in aquaculture waste deposition modelling. Aquacult Environ Interact 12:401–415

Ådlandsvik B, Sundby S (1994) Modelling the transport of cod larvae from the Lofoten area. ICES Mar Sci Symp 198:379–392

Asplin L, Albretsen J, Johnsen IA, Sandvik AD (2020) The hydrodynamic foundation for salmon lice dispersion modeling along the Norwegian coast. Ocean Dyn 70: 1151–1167

Baeverfjord G, Krogdahl A (1996) Development and regression of soybean meal induced enteritis in Atlantic salmon, *Salmo salar* L., distal intestine: a comparison with the intestines of fasted fish. J Fish Dis 19:375–387

Bannister RJ, Johnsen IA, Hansen PK, Kutti T, Asplin L (2016) Near- and far-field dispersal modelling of organic waste from Atlantic salmon aquaculture in fjord systems. ICES J Mar Sci 73:2408–2419

Bokulich NA, Kaehler BD, Rideout JR, Dillon M and others (2018) Optimizing taxonomic classification of marker-gene amplicon sequences with QIIME 2's q2-feature-classifier plugin. Microbiome 6:90

Borja A, Franco J, Perez V (2000) A marine biotic index to establish the ecological quality of soft-bottom benthos within European estuarine and coastal environments. Mar Pollut Bull 40:1100–1114

Borja A, Rodríguez JG, Black K, Bodoy A and others (2009) Assessing the suitability of a range of benthic indices in the evaluation of environmental impact of fin and shellfish aquaculture located across Europe. Aquaculture 293: 231–240

Bravo F, Grant J (2018) Modelling sediment assimilative capacity and organic carbon degradation efficiency at marine fish farms. Aquacult Environ Interact 10:309–328

Broch OJ, Daae RL, Ellingsen IH, Nepstad R, Bendiksen EÅ, Reed JL, Senneset G (2017) Spatiotemporal dispersal and deposition of fish farm wastes: a model study from Central Norway. Front Mar Sci 4:199

Brooks KM, Mahnken CVW (2003) Interactions of Atlantic salmon in the Pacific northwest environment: II. Organic wastes. Fish Res 62:255–293

Brooks KM, Mahnken C, Nash C (2002) Environmental effects associated with marine netpen waste with emphasis on salmon farming in the Pacific northwest. In: Stickney RR, McVey JP (eds) Responsible marine aquaculture. CABI Publishing, Wallingford, p 159–203

Burow LC, Woebken D, Marshall IPG, Singer SW and others (2014) Identification of *Desulfobacterales* as primary hydrogenotrophs in a complex microbial mat community. Geobiology 12:221–230

Callahan BJ, McMurdie PJ, Rosen MJ, Han AW, Johnson AJA, Holmes SP (2016) DADA2: high-resolution sample inference from Illumina amplicon data. Nat Methods 13: 581–583

Carvajalino-Fernández MA, Keeley NB, Fer I, Law BA, Bannister RJ (2020a) Effect of substrate type and pellet age on the resuspension of Atlantic salmon faecal material. Aquacult Environ Interact 12:117–129

Carvajalino-Fernández MA, Sævik PN, Johnsen IA, Albretsen J, Keeley NB (2020b) Simulating particle organic matter dispersal beneath Atlantic salmon fish farms using different resuspension approaches. Mar Pollut Bull 161:111685

Chamberlain J, Stucchi D (2007) Simulating the effects of parameter uncertainty on waste model predictions of marine finfish aquaculture. Aquaculture 272:296–311

Chen YS, Beveridge MCM, Telfer TC (1999) Physical characteristics of commercial pelleted Atlantic salmon feeds and consideration of implications for modeling of waste dispersion through sedimentation. Aquacult Int 7:89–100

Chen YS, Beveridge MCM, Telfer TC, Roy WJ (2003) Nutrient leaching and settling rate characteristics of the faeces of Atlantic salmon (*Salmo salar* L.) and the implications for modelling of solid waste dispersion. J Appl Ichthyol 19: 114–117

Cranford P, Brager L, Elvines D, Wong D, Law B (2020) A revised classification system describing the ecological quality status of organically enriched marine sediments based on total dissolved sulfides. Mar Pollut Bull 154: 111088

Cromey CJ, Nickell TD, Black KD (2000) DEPOMOD. A model for predicting the effects of solids deposition from mariculture to the benthos. The Scottish Association for Marine Science, Oban

Cromey CJ, Nickell TD, Black KD (2002) DEPOMOD — modelling the deposition and biological effects of waste solids from marine cage farms. Aquaculture 214:211–239

Cromey CJ, Thetmeyer H, Lampadariou N, Black KD, Kögeler J, Karakassis I (2012) MERAMOD: predicting the deposition and benthic impact of aquaculture in the eastern Mediterranean Sea. Aquacult Environ Interact 2:157–176

Cubillo AM, Ferreira JG, Robinson SMC, Pearce CM, Corner RA, Johansen J (2016) Role of deposit feeders in integrated multi-trophic aquaculture — a model analysis. Aquaculture 453:54–66

Droppo IG, Jaskot C, Nelson T, Milne J, Charlton M (2007) Aquaculture waste sediment stability: implications for waste migration. Water Air Soil Pollut 183:59–68

Elvines DM, Smeaton M, Ross DJ, White CA and others (2024) Performance of biochemical tools as fish waste particle tracers in a dispersive marine system. Ecol Indic 158:111474

Fox C, Webb C, Grant J, Brain S, Fraser S, Abell R, Hicks N (2023) Measuring and modelling the dispersal of salmon farm organic waste over sandy sediments. Aquacult Environ Interact 15:251–269

Frühe L, Dully V, Forster D, Keeley NB and others (2021) Global trends of benthic bacterial diversity and community composition along organic enrichment gradients of salmon farms. Front Microbiol 12:637811

Giles H (2008) Using Bayesian networks to examine consistent trends in fish farm benthic impact studies. Aquaculture 274:181–195

Haidvogel DB, Arango H, Budgell WP, Cornuelle BD and others (2008) Ocean forecasting in terrain-following coordinates: formulation and skill assessment of the Regional Ocean Modeling System. J Comput Phys 227: 3595–3624

Hargrave BT, Holmer M, Newcombe CP (2008) Towards a classification of organic enrichment in marine sediments based on biogeochemical indicators. Mar Pollut Bull 56: 810–824

Hartstein ND, de Young B, Anderson MR, Maxey JD (2021) Hydrodynamic implications in and around a caged finfish farm and its implications on the dispersal of farm debris. Aquacult Eng 93:102154

Hill PS (1996) Sectional and discrete representations of floc breakage in agitated suspensions. Deep Sea Res I 43: 679–702

Hill PS, Newgard JP, Law BA, Milligan TG (2013) Flocculation on a muddy intertidal flat in Willapa Bay, Washington, Part II: observations of suspended particle size in a secondary channel and adjacent flat. Cont Shelf Res 60: S145–S156

Hu H, Kortner TM, Gajardo K, Chikwati E, Tinsley J, Krogdahl Å (2016) Intestinal fluid permeability in Atlantic salmon (*Salmo salar* L.) is affected by dietary protein source. PLOS ONE 11:e0167515

Jørgensen BB, Findlay AJ, Pellerin A (2019) The biogeochemical sulfur cycle of marine sediments. Front Microbiol 10:849

Katoh K, Standley DM (2013) MAFFT multiple sequence alignment software version 7: improvements in performance and usability. Mol Biol Evol 30:772–780

Kawahara N, Shigematsu K, Miyadai T, Kondo R (2009) Comparison of bacterial communities in fish farm sediment along an organic enrichment gradient. Aquaculture 287:107–113

Keeley NB, Forrest BM, Crawford C, Macleod CK (2012) Exploiting salmon farm benthic enrichment gradients to evaluate the regional performance of biotic indices and environmental indicators. Ecol Indic 23:453–466

Keeley NB, Forrest BM, MacLeod CK (2013a) Novel observations of benthic enrichment in contrasting flow regimes with implications for marine farm monitoring and management. Mar Pollut Bull 66:105–116

Keeley NB, Cromey CJ, Goodwin EO, Gibbs MT, Macleod CM (2013b) Predictive depositional modelling (DEPOMOD) of the interactive effect of current flow and resuspension on ecological impacts beneath salmon farms. Aquacult Environ Interact 3:275–291

Keeley N, Wood SA, Pochon X (2018) Development and preliminary validation of a multi-trophic metabarcoding biotic index for monitoring benthic organic enrichment. Ecol Indic 85:1044–1057

Keeley N, Valdemarsen T, Woodcock S, Holmer M, Husa V, Bannister R (2019) Resilience of dynamic coastal benthic ecosystems in response to large-scale finfish farming. Aquacult Environ Interact 11:161–179

Keeley N, Valdemarsen T, Strohmeier T, Pochon X, Dahlgren T, Bannister R (2020) Mixed-habitat assimilation of organic waste in coastal environments — It's all about synergy! Sci Total Environ 699:134281

Keeley N, Laroche O, Birch M, Pochon X (2021) A substrate-independent benthic sampler (SIBS) for hard and mixed-bottom marine habitats: a proof-of-concept study. Front Mar Sci 8:627687

Kinoshita K, Tamaki S, Yoshioka M, Srithonguthai S and others (2008) Bioremediation of organically enriched sediment deposited below fish farms with artificially mass-cultured colonies of a deposit-feeding polychaete *Capitella* sp. I. Fish Sci 74:77–87

Klindworth A, Pruesse E, Schweer T, Peplies J, Quast C, Horn M, Glöckner FO (2013) Evaluation of general 16S ribosomal RNA gene PCR primers for classical and next-generation sequencing-based diversity studies. Nucleic Acids Res 41:e1

Kozich JJ, Westcott SL, Baxter NT, Highlander SK, Schloss PD (2013) Development of a dual-index sequencing strategy and curation pipeline for analyzing amplicon sequence data on the MiSeq Illumina sequencing platform. Appl Environ Microbiol 79:5112–5120

Kristensen E, Holmer M (2001) Decomposition of plant materials in marine sediment exposed to different electron acceptors (O_2, NO_3^-, and SO_4^{2-}), with emphasis on substrate origin, degradation kinetics, and the role of bioturbation. Geochim Cosmochim Acta 65:419–433

Kutti T, Hansen PK, Ervik A, Høisæter T, Johannessen P (2007) Effects of organic effluents from a salmon farm on a fjord system. II. Temporal and spatial patterns in infauna community composition. Aquaculture 262:355–366

La Rosa T, Mirto S, Mazzola A, Danovaro R (2001) Differential responses of benthic microbes and meiofauna to fish-farm disturbance in coastal sediments. Environ Pollut 112:427–434

Law BA, Hill PS, Maier I, Milligan TG, Page F (2014) Size, settling velocity and density of small suspended particles at an active salmon aquaculture site. Aquacult Environ Interact 6:29–42

Law BA, Hill PS, Milligan TG, Zions V (2016) Erodibility of aquaculture waste from different bottom substrates. Aquacult Environ Interact 8:575–584

Lozupone C, Knight R (2005) UniFrac: a new phylogenetic method for comparing microbial communities. Appl Environ Microbiol 71:8228–8235

Lynch DR, Greenberg DA, Bilgili A, McGillicuddy DJ Jr, Manning JP, Aretxabaleta AL (2014) Particles in the coastal ocean: theory and applications. Cambridge University Press, New York, NY

Magill SH, Thetmeyer H, Cromey CJ (2006) Settling velocity of faecal pellets of gilthead sea bream (*Sparus aurata* L.) and sea bass (*Dicentrarchus labrax* L.) and sensitivity analysis using measured data in a deposition model. Aquaculture 251:295–305

Martin SJ, Mather C, Knott C, Bavington D (2021) 'Landing' salmon aquaculture: ecologies, infrastructures and the promise of sustainability. Geoforum 123:47–55

McCaig AE, Phillips CJ, Stephen JR, Kowalchuk GA and others (1999) Nitrogen cycling and community structure of proteobacterial β-subgroup ammonia-oxidizing bacteria within polluted marine fish farm sediments. Appl Environ Microbiol 65:213–220

Milligan TG, Law BA (2013) Contaminants at the sediment–water interface: implications for environmental impact assessment and effects monitoring. Environ Sci Technol 47:5828–5834

Oksanen J, Simpson G, Blanchet F, Kindt R and others (2022) vegan: community ecology package. R package version 2.6-4. https://CRAN.R-project.org/package=vegan

Paerl HW, Pinckney JL (1996) A mini-review of microbial

consortia: their roles in aquatic production and biogeochemical cycling. Microb Ecol 31:225–247

Papageorgiou N, Kalantzi I, Karakassis I (2010) Effects of fish farming on the biological and geochemical properties of muddy and sandy sediments in the Mediterranean Sea. Mar Environ Res 69:326–336

Pochon X, Wood SA, Keeley NB, Lejzerowicz F, Esling P, Drew J, Pawlowski J (2015) Accurate assessment of the impact of salmon farming on benthic sediment enrichment using foraminiferal metabarcoding. Mar Pollut Bull 100:370–382

Pochon X, Wood S, Atalah J, Laroche O, Zaiko A, Keeley N (2020) A validated protocol for benthic monitoring of New Zealand's salmon farms using environmental DNA. Prepared for Seafood Innovation Ltd, New Zealand King Salmon Company Ltd, Ministry for Primary Industries and Marlborough District Council. Cawthron Rep No. 3400. Cawthron Institute, Nelson

Price MN, Dehal PS, Arkin AP (2010) FastTree 2 — approximately maximum-likelihood trees for large alignments. PLOS ONE 5:e9490

Quast C, Pruesse E, Yilmaz P, Gerken J and others (2013) The SILVA ribosomal RNA gene database project: improved data processing and web-based tools. Nucleic Acids Res 41:D590–D596

Rygg B, Norling K (2013) Norwegian Sensitivity Index (NSI) for marine macroinvertebrates, and an update of Indicator Species Index (ISI). NIVA-rapport: 6475. Norsk institutt for vannforskning, Oslo

Sara G, Scilipoti D, Mazzola A, Modica A (2004) Effects of fish farming waste to sedimentary and particulate organic matter in a southern Mediterranean area (Gulf of Castellammare, Sicily): a multiple stable isotope study ($\delta^{13}C$ and $\delta^{15}N$). Aquaculture 234:199–213

Shchepetkin AF, McWilliams JC (2005) The regional oceanic modeling system (ROMS): a split-explicit, free-surface, topography-following-coordinate oceanic model. Ocean Model 9:347–404

Smeaton M, Vennell R (2020) A comparison of three depositional models: DEPOMOD, SMTOMOD and VenOM. Cawthron Rep No. 3336. Cawthron Institute, Nelson

Standards Norway (2016) Environmental monitoring of benthic impact from marine fish farms. NS 9410:2016. Standards Norway, Oslo

Stoeck T, Frühe L, Forster D, Cordier T, Martins CIM, Pawlowski J (2018) Environmental DNA metabarcoding of benthic bacterial communities indicates the benthic footprint of salmon aquaculture. Mar Pollut Bull 127: 139–149

Svensson SGB, Strohmeier T, Rastrick H, Garcia AA, Lock EJ, Sveier H, Jansen HM (2023) Life history traits for *Ophryotrocha craigsmithi* (Wiklund, Glover & Dahlgren, 2009), a candidate species in integrated multitrophic aquaculture. Front Mar Sci 10:1116765

Valdemarsen T, Kristensen E, Holmer M (2010) Sulfur, carbon, and nitrogen cycling in faunated marine sediments impacted by repeated organic enrichment. Mar Ecol Prog Ser 400:37–53

Vandamme P, Pot B, Falsen E, Kersters K, Devreise LA (1996) Taxonomic study of Lancefield streptococcal groups C, G, and L (*Streptococcus dysgalactiae*) and proposal of *S. dysgalactiae* subsp. *equisimilis* subsp. nov. Int J Syst Bacteriol 46:774–781

Vennell R, Scheel M, Weppe S, Knight B, Smeaton M (2021) Fast lagrangian particle tracking in unstructured ocean model grids. Ocean Dyn 71:423–437

Vezzulli L, Chelossi E, Riccardi G, Fabiano M (2002) Bacterial community structure and activity in fish farm sediments of the Ligurian sea (Western Mediterranean). Aquacult Int 10:123–141

Wang Q, Garrity GM, Tiedje JM, Cole JR (2007) Naïve Bayesian classifier for rapid assignment of rRNA sequences into the new bacterial taxonomy. Appl Environ Microbiol 73:5261–5267

Wiese J, Thiel V, Gärtner A, Schmaljohann R, Imhoff JF (2009) *Kiloniella laminariae* gen. nov., sp. nov., an alphaproteobacterium from the marine macroalga *Laminaria saccharina.* Int J Syst Evol Microbiol 59:350–356

Woodcock SH, Strohmeier T, Strand Ø, Olsen SA, Bannister RJ (2018) Mobile epibenthic fauna consume organic waste from coastal fin-fish aquaculture. Mar Environ Res 137:16–23

Editorial responsibility: Dror Angel, Haifa, Israel
Reviewed by: Y. Olsen, F. Bravo and 1 anonymous referee
Submitted: March 15, 2024; Accepted: October 29, 2024
Proofs received from author(s): December 16, 2024